AN UPDATED COMPUTER MODEL OF MONTSERRAT GEOTHERMAL FIELD

Marijn van den Heuvel[1], Maella Bremaud[2], Mike O'Sullivan[3], John O'Sullivan[3], Joris Popineau[3], Susana Guzman[3], Michael Gravatt[3] and Graham A. Ryan[4,5]

[1]Department of Mechanical Engineering, Eindhoven University of Technology, The Netherlands

[2]Ecole nationale supérieure de géologie, Université de Lorraine, France

[3]Department of Engineering Science, University of Auckland, Auckland, New Zealand

[4]Montserrat Volcano Observatory, Flemmings, Montserrat, W.I.

[5]Seismic Research Center, University of the West Indies, St. Augustine, Trinidad and Tobago, West Indies.
m.osullivan@auckland.ac.nz

Keywords: *Montserrat, geothermal model, natural state, inverse modelling*

ABSTRACT

The model of the geothermal field on Montserrat Island, developed at the University of Auckland in 2018, has been updated in the following three ways. First, the model grid was extended to the south-east to include more of the area around the Soufrière Hills Volcano, and the grid was refined. Secondly, temperatures inferred from a seismic velocity anomaly model (Ryan & Shalev, 2014) were included in the suite of data to be used for model calibration. Thirdly, three software packages were used for parameter estimation with the natural state model, namely: iTOUGH2, PEST and iWaiwera. iWaiwera uses the adjoint method to evaluate derivatives efficiently and therefore it was able to very quickly estimate a large number of model parameters.

A good match to the downhole temperatures in wells Mon-1 and Mon-2 was obtained as well as a good match to the inferred temperatures at three elevations.

1. INTRODUCTION

1.1 Montserrat

Montserrat is a small island, a British Overseas Territory located in the Lesser Antilles region of the Caribbean archipelago. The Lesser Antilles islands are dominated by volcanoes, and so many of them have potential for geothermal energy production. For instance, the French Island of Guadeloupe (the neighbouring country to Montserrat), is currently running a geothermal power plant with a total capacity of 15 MWe. Montserrat has a total area about 102 km^2 and is approximately 16 km long and 11 km wide. It has an active volcano, the Soufrière Hills Volcano, which is located in the south of the island and last erupted in 1995 (Brophy et al., 2014; Ryan & Shalev, 2014; Kokelaar, 2002).

The existing electrical load for Montserrat is about 2 MWe, and, apart from approximately 250 kW of installed solar photovoltaic generation capacity, the government are currently dependent on fossil fuels for generating electricity at a much higher operational cost than geothermal energy (Ryan & Shalev, 2014). Since this island has geothermal potential, the government have been investigating the possibility of using geothermal energy to fulfil their electricity requirements.

In 2009, EGS Inc., a US geothermal exploration company, was asked by the government of Montserrat to conduct preliminary surveys of geology, geophysics and geochemistry to assess the feasibility of developing geothermal energy in Montserrat.

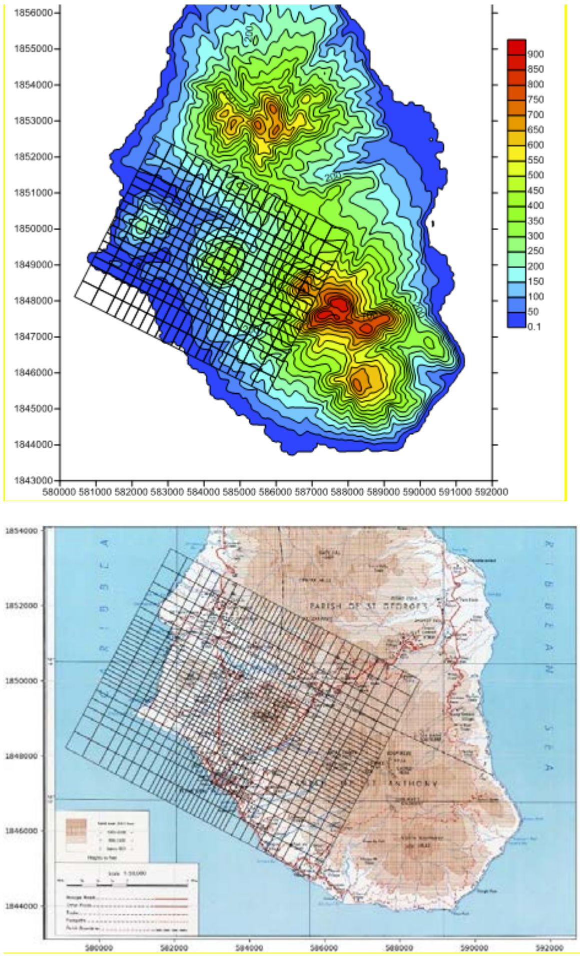

Figure 1: Map of Montserrat showing the topography and: (Top) the grid for model MO8159 (from Sumantoro, 2014), (Bottom) the grid for model MO24535.

However, exploration of the geothermal resources in Montserrat is limited by on-going eruptions of the Soufrière Hills Volcano. From a safety standpoint, it is too risky to develop a geothermal project on the flanks of a regularly active volcano (EGS, 2010). The 1995 eruption had a huge impact on Montserrat, as it destroyed the ex-capital city, Plymouth, and left around 30% of the island uninhabitable.

Proceedings 42nd New Zealand Geothermal Workshop
24-26 November 2020
Waitangi, New Zealand
ISSN 2703-4275

EGS (2010) explained that from a geologic, logistics and safety perspective, the best possible location for developing a geothermal system is the area neighbouring St. George's Hill and Garibaldi Hill because these areas are unlikely to be directly affected by pyroclastic density currents from the volcano.

So far, three exploration wells, Mon-1, Mon-2 and Mon-3, have been drilled and temperature profiles were obtained from the first two, whose locations are shown in Figure 3

1.2 Modelling plan

In two previous studies (Sumantoro, 2014; Lehuger et al., 2018), we developed computer models based on a conceptual model and calibrated them using the measured temperature profiles for wells Mon-1 and Mon-2 (no profile is available from the third well Mon-3). However, because of the small amount of data available, there were not many constraints on the permeability structure of the models.

The aim of the present study is to extend the 2018 study by including temperatures inferred from the seismic tomography study of Ryan & Shalev (2014) as part of the suite of calibration data. The other point of difference with the earlier studies is that here we make extensive use of automatic calibration (inverse modelling) methods, whereas the 2014 study used only manual calibration and the 2018 study used mostly manual calibration. In the present study, inverse modelling is carried out with three different software packages, iTOUGH2, PEST and iWaiwera. These software packages are discussed further in later sections.

2. COMPUTER MODEL DESIGN

2.1 Model grid

Four models will be discussed below: one each from the 2014 and 2018 studies and two from the present study. Their details are given in Table 1. The grids for models MO8159 and MO245335 are shown in Figure 1, superimposed on topographical maps of Montserrat.

Table 1: Model details.

Name	Columns	Layers	Blocks (Area)	ID
2014 model	320 (20×16)	29	8159 (6km × 5km)	MO8159
2018 model	672 (28×24)	29	16587 (7km × 6km)	MO16587
Initial model	980 (35×28)	29	24535 (7.5km × 6km)	MO24535
Final model	980 (35×28)	40	27660 (7.5km × 6km)	MO27660

For the later models, the grid was increased in size and the model was refined near the wells. Plan views of the grids for MO16587 and MO24535 are shown in Figure 2 and Figure 3, respectively. These two plots also show the faults that are explicitly included in the models. As noted in Table 1, models MO24535 and MO27660 use the same column structure.

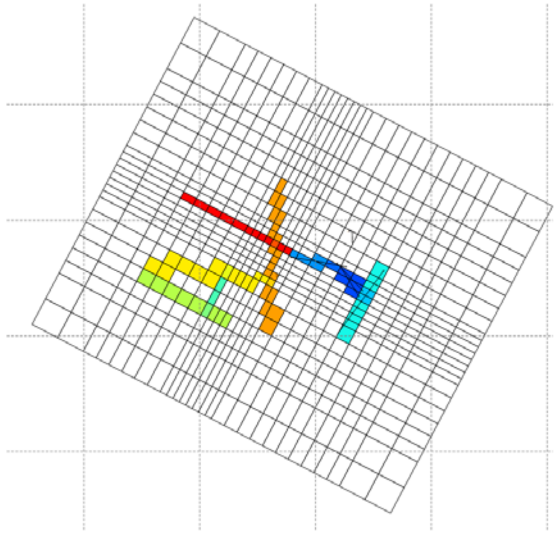

Figure 2: Plan view of the grid for model MO16587.

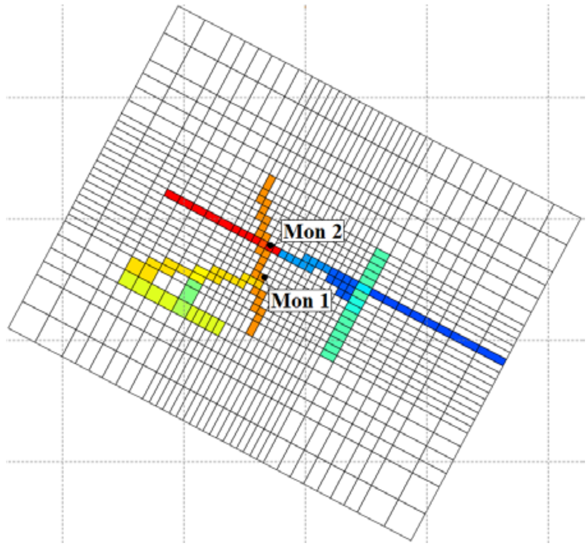

Figure 3: Plan view of the grid for model MO24535 and model MO27660.

The same layer structure (shown in Figure 4) was used in models MO16587 and MO24535. For model MO27660, the layers were refined around the water table elevation (see Figure 5). There were two reasons for this: first to better resolve the water table location and, secondly, to produce a Waiwera-compatible model with all layers being complete at the top of each column. AUTOUGH2 allows the block at the top of a column to be less than the nominated layer thickness (to better follow the topography) where as in Waiwera the block thickness has to match the layer thickness.

Simulations were carried out with AUTOUGH2 (Yeh et al., 2012) (the University of Auckland version of the TOUGH2 simulator (Pruess et al., 1999)) and with Waiwera (Croucher et al., 2020), a simulator developed at the University of Auckland in collaboration with GNS Science. As noted above, TOUGH2 allows for incomplete layers at the top of columns whereas Waiwera does not.

2.2 Conceptual model

Most aspects of the conceptual model are unchanged from the 2018 study (Lehuger et al., 2018) and are not discussed here. It is discussed further by van den Heuvel (2019) and Bremaud (2019) who also implemented the conceptual model in LeapFrog (Alcaraz et al., 2011).

The main problem with model MO16587 was that the deep hot upflow was too far west and the match to the inferred seismic temperatures (Ryan & Shalev, 2014) was poor. To address this issue the lineament corresponding to the volcanic vent alignment identified by EGS Inc. (2010) was extended further to the SE (see Figure 3). This allows for hot upflow further east, even under the Soufrière Hill Volcano (but in fact, in the final model, the main upflow is beneath St. Georges Hill).

2.3 Geological model

The 2014 model (MO8159) had a very simple three-layer geological structure. For model MO16587, and subsequently for MO245353, the middle geological formation used in MO8159 was sub-divided into three geological formations. Also, the faults were explicitly included in the model by having their own rock-types assigned (see Figures 2 and 4). Further complexity was introduced by allowing the intersection of two faults to have its own rock-type.

The rock-type structure of MO16587 was maintained at first for MO24535 (see Figure 4) but later and during the calibration of MO27660 further sub-division of some formations was carried out and offset was introduced across the NS fault (see Figure 5).

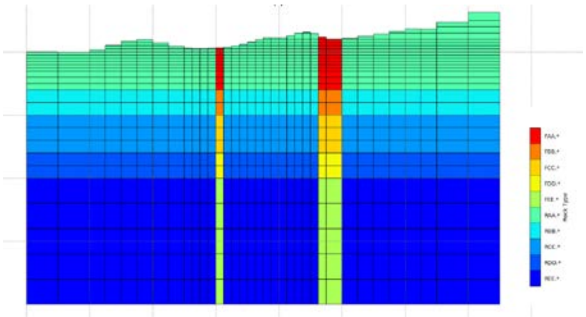

Figure 4: A vertical slice showing the initial geological model for model MO24535.

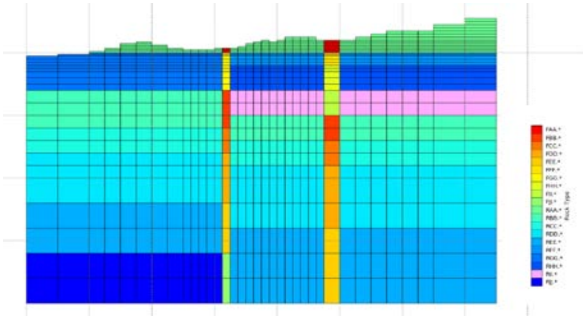

Figure 5: A vertical slice showing the final geological model for model MO27660.

2.4 Structural model

The faults shown in Figures 2 and 3 are based on the EGS (2010) review (see Figure 6) and a later review by Rowland & Ryan (2014) (see Figure 7). The structural model is discussed further in Lehuger et al., (2018).

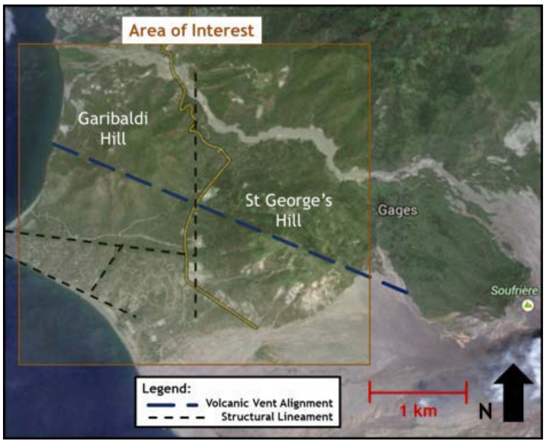

Figure 6: Fault lineaments in the St George's Hill/Garibaldi Hill Area (modified after EGS, 2010).

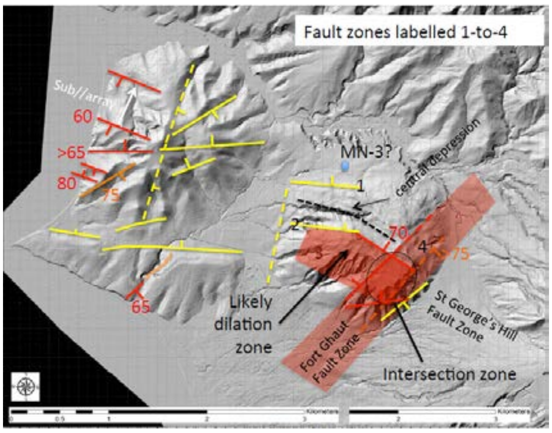

Figure 7: Fault lineaments in the St George's Hill/Garibaldi Hill Area (from Rowland & Ryan, 2014). Red- confident. Orange- some uncertainty with respect to strike, dip, or dip direction of controlling structure (dashed if inferred based on nearby field observations). Yellow- unsupported by field data, but likely, based on geomorphic expression (dashed if more speculative).

2.5 Boundary conditions

<u>Sides.</u> The sides of the model are set as no-flow boundaries for heat and mass.

<u>*Base*</u>. At the base of the model, a background heat flow of 100 mW/m^2 is set. Then several upflows of hot water with enthalpies of 1250 kJ/kg are added at the base of the faults. The values for the mass flow rates are based on the conceptual model but are changed during the calibration process.

<u>*Top surface*</u>. The unsaturated zone is included in the model and an air-water equation of stste (EOS3) is used. Therefore, an atmospheric pressure 1.0135 bar and a temperature of 28°C are set at the surface together with an air mass fraction of 0.999825, corresponding to almost dry air. Also, rainfall is included by the injection of water at the top of the model at a temperature of 28°C. The infiltration rate corresponds to 10% of the annual rainfall of 1000 mm/year. For the columns under the ocean, the top boundary pressure is set to the hydrostatic pressure corresponding to the depth of the ocean,

but based on a freshwater density of 996.2 kg/m^3. The temperatures of the corresponding top boundary blocks are set to 28°C.

2.6 Calibration data

The only hard data are the downhole temperature profiles for wells Mon-1 and Mon-2. These are shown in Figure 8, together with the best results achieved with the final version of MO16587 (very similar to results from the partly calibrated model MO24535V2).

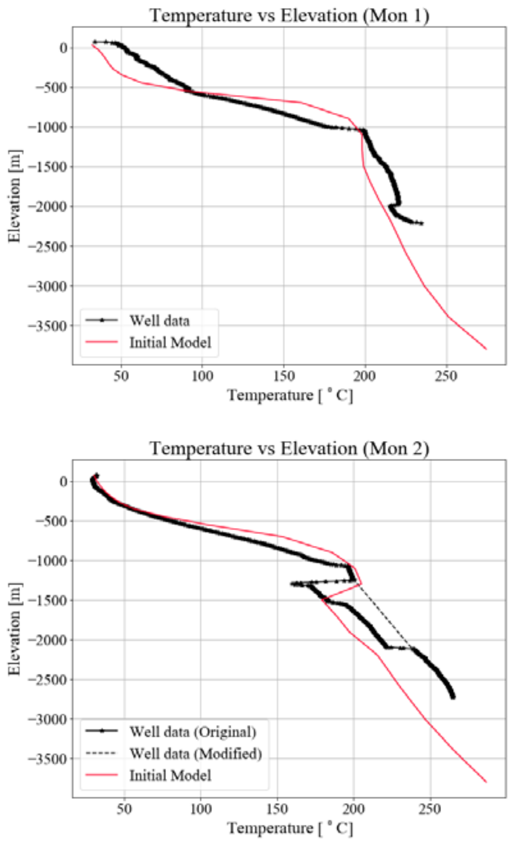

Figure 8: Downhole temperature profiles for wells Mon-1 and Mon-2. Measured data vs results from the final version of MO16587 (very similar to results from model MO24535V2).

The second type of calibration data used are the temperatures inferred from the seismic velocity anomaly model produced by Ryan & Shalev (2014). These are shown in Figure 9.

Although the matches achieved with model MO16587 to the downhole temperatures are very good (see Figure 8), the match to the inferred seismic temperatures is poor. As shown in Lehuger et al. (2018) the hot upflow in model MO16587 was probably 1-2 km too far west.

Finally, three significant surface features were identified from the EGS (2010) study (see Table 2) and their temperatures were added as targets to be matched by the surface temperatures in the model.

The areas of the surface features are small compared to the area of a model block and therefore it is expected that the model surface temperatures may be lower than the measured values in Table 2.

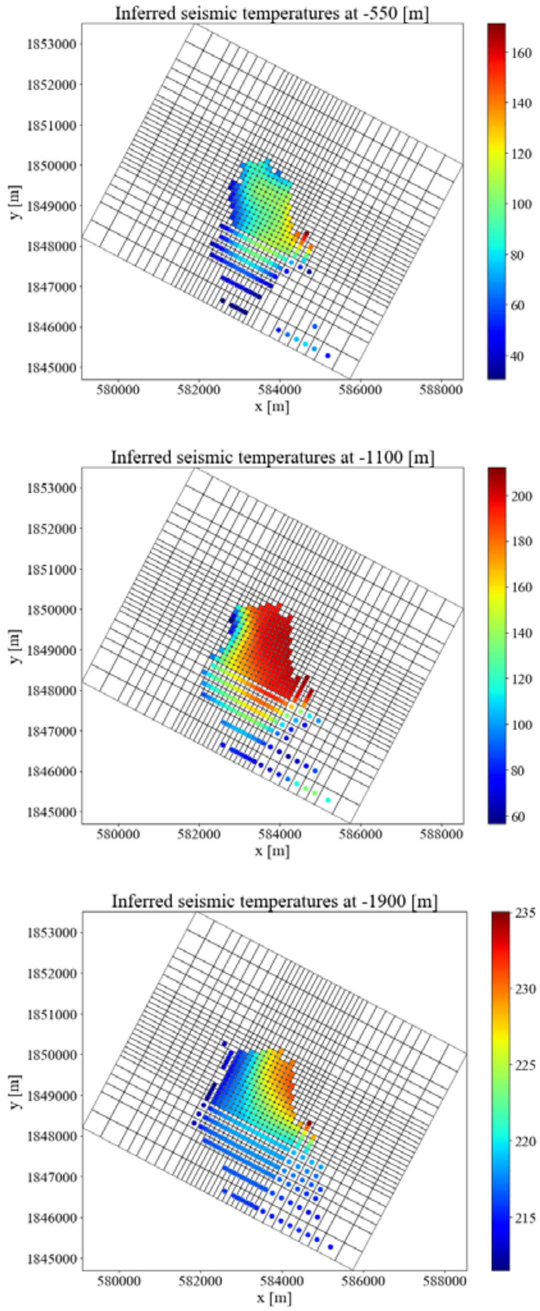

Figure 9: Estimated temperatures (°C) at three elevations from the seismic velocity anomaly model by (Ryan & Shalev, 2014).

Table 2: Significant surface features.

Name	ID	Model column	Temperature
Hot Water Pond	MHP-1	er	59.3°C
Sturges Park well	STG-55	ew	38.3°C
Gages Soufrière spring 7	-	mj	95.4°C

The temperature in Table 2, given by EGS (2010), for Hot Water Pond may be too low as other investigations have suggested values close to boiling (Chiodini et al., 1996; Geotermica Italiana, 1991). Also, the Gages Soufrière spring 7 has been covered by recent eruptions.

3. INVERSE MODELLING

3.1 Theory

The aim of inverse modelling or automatic calibration is to optimise the model parameters so that the model results match the observation data (Gonzalez-Gutierrez et al., 2018). The observation data usually comes from measured data only, however, for this study of Montserrat, only limited measured data are available, and therefore inferred temperatures from seismic data (see Figure 9) are also used as observed data.

There are several key elements for inverse modelling software. First, forward modelling software is required. Secondly, an objective function which measures the misfit between the model output and the observed data should be set up, and thirdly, a minimization algorithm which reduces the objective function by automatically updating parameter values must be implemented (Finsterle, 2015). As mentioned above for the first key element, the forward modelling software, we use either AUTOUGH2 or Waiwera. The mathematical formulation of the second and third steps can be expressed as a constrained optimization problem:

$$\min f(p) \text{ such that } g(p) = 0 \qquad (1)$$

Here p are the parameters to calibrate and the constraint $g(p) = 0$ represents the equations solved by the forward model. For geothermal reservoir modelling, these equations are non-linear mass and energy transport equations.

The objective function can be expressed in the form of a regularized sum of squares as follows (Gonzalez-Gutierrez et al., 2018):

$$f(p) = \|W_1(d(p) - d_{obs})\|^2 + \alpha f_p(p) \qquad (2)$$

Here W_1 is the observation weighting matrix, $d(p)$ are the model results, d_{obs} are the observed data, and α is the regularization parameter multiplying some regularization measure f_p.

If we define the observation residuals by

$$r(p) = d(p) - d_{obs} \qquad (3)$$

Then we can rewrite (2) as

$$f(p) = f_d(p) + \alpha f_p(p) \qquad (4)$$

Where

$$f_d(p) = \|W_1 r(p)\|^2 \qquad (5)$$

In order to apply a gradient-based minimization algorithm, of the kind that is available in iTOUGH2, PEST and iWaiwera, the sensitivity matrix (or Jacobian) containing derivatives of $r(p)$ with respect to the parameters p must be calculated. The way this is done differs between the various inverse modelling software.

3.2 iTOUGH2

The iTOUGH2 software package provides inverse modelling capabilities for TOUGH2 models. One of the key features of iTOUGH2 compared to other inverse modelling software is its extensive error analysis, which provides statistical information about residuals and estimation uncertainties (Finsterle, 2015). This feature was not used to its full capability with the current Montserrat model but might be useful in the future if more data become available.

For manual calibration of all models we used the AUTOUGH2 simulator but for the iTOUGH2 runs we swapped to using the inbuilt version of TOUGH2. With the right settings of some of the solver options it performs almost as well as AUTOUGH2.

The objective function as presented in (2) includes a regularization term. However, for the iTOUGH2 simulations regularization was not included and therefore, the objective function reduces to:

$$f(p) = f_d(p) = \|W_1 r(p)\|^2 \qquad (6)$$

In iTOUGH2 the gradient-based, Levenberg-Marquardt method is the default minimization method and is the one we use here. It requires the calculation of the sensitivity matrix, or Jacobian, containing the derivatives of $r(p)$ with respect to p and for this calculation iTOUGH2 uses the finite differencing method, which requires the forward model to be run over and over, making the process very computationally intensive. As a result, iTOUGH2 runs very slowly and for the Montserrat model it takes of the order of 1–2 days to run one iTOUGH2 iteration. These derivatives are then used within the minimization algorithm.

More details about the way the iTOUGH2 software works and the full list of commands, are available, respectively, from the User Manual (Finsterle, 2007) and the Command Reference Manual (Finsterle, 2015).

3.3 PEST

PEST offers the capability of inverse modelling with any type of forward model. It can interact with all sorts of models without requiring changes to their input and output files. Another feature is that it has many options that can be used during the calibration process. For example, singular value decomposition (SVD) and Tikhonov regularization (see *PEST - The book* (Doherty, 2015) or the freely available *User Manual* (Doherty, 2018a, 2018b), for more details).

Nevertheless, by default PEST uses the Levenberg-Marquadt method and uses finite differencing in order to calculate the derivatives of $r(p)$ with respect to p and thus still needs to run the forward model many times in order to estimate the parameters, making it similar in speed to iTOUGH2 but still rather slow compared to iWaiwera.

Note that users can provide PEST with functions to calculate derivatives, e.g., using adjoint-based code as implemented in Bjarkason et al. (2019). This option is worth considering as a modification to the standard PEST approach.

The standard version of PEST requires three types of input files, namely: template files, instruction files and a control file. At the University of Auckland, we have developed a modified approach, named "goPEST", which uses two simpler input files and then applies python scripts to build the standard PEST files (see van den Heuvel, 2019).

3.4 iWaiwera

iWaiwera is a Python 3.x interface created at the University of Auckland for solving inverse problems where Waiwera is used for the forward model. The key feature of iWaiwera is that it uses the so-called adjoint method (Bjarkason et al., 2019, 2018, 2016) instead of finite differencing to calculate derivatives. Various options for minimization provided by the SciPy library are offered in iWaiwera but not the Levenberg-Marquardt method. Instead we used the Newton conjugate gradient method (Newton CG). The simpler the limited memory BFGS algorithm was also tested but the Newton CG method gave faster convergence and was preferred. The latter requires the evaluation of the sensitivity matrix containing derivatives of residuals with respect to model parameters whereas the former requires just the derivatives of the objective function obtained by differentiating (2):

$$\frac{df}{dp} = 2\left(\frac{dr}{dp}\right)^T W_1^T W_1 r + \alpha \frac{df_p}{dp} \qquad (7)$$

The adjoint method provides an analytical procedure for calculating either the sensitivity matrix or the total derivative of the objective function. It uses the method of Lagrange multipliers to implement the adjoint method (Gonzalez-Gutierrez et al., 2018; Bjarkason et al. 2019). Hence, there is no need to run the forward model many times to evaluate derivatives of model outputs, making it computationally much faster than applying finite differencing. This speed-up is especially significant for calibrating natural state models (see Bjarkason et al. 2019).

Currently, there are two forms of regularization implemented within the iWaiwera software: simple regularization based on the prior choice of parameters and a smoothing regularization when stronger regularization is required. For the current study the former was used.

4. IMPLEMENTATION AND RESULTS

4.1 Initial model

The first stage of modelling involved transferring over model MO16587 to the new grid structure (see Figures 3 and 4) while maintaining essentially the same geological structure (see Figure 4) and the same deep upflows (model MO24535V1). Then some manual calibration and an initial run with iTOUGH2 were carried out to produce model MO24535V2. As shown in Figure 8, the temperature profiles for wells Mon-1 and Mon-2 are quite well matched by this model, however, the match to the inferred seismic temperatures is poor. The differences between the model results and inferred seismic temperatures are shown in Figure 10.

The plots show that the hot reservoir in the initial model is too far west, the temperature at -550 m is generally too high and at -1900 m is generally too low. There are only irregular patches of the seismic data available and it is based on a model itself and is thus not directly measured data. However, it is very useful in constraining the structure of the model.

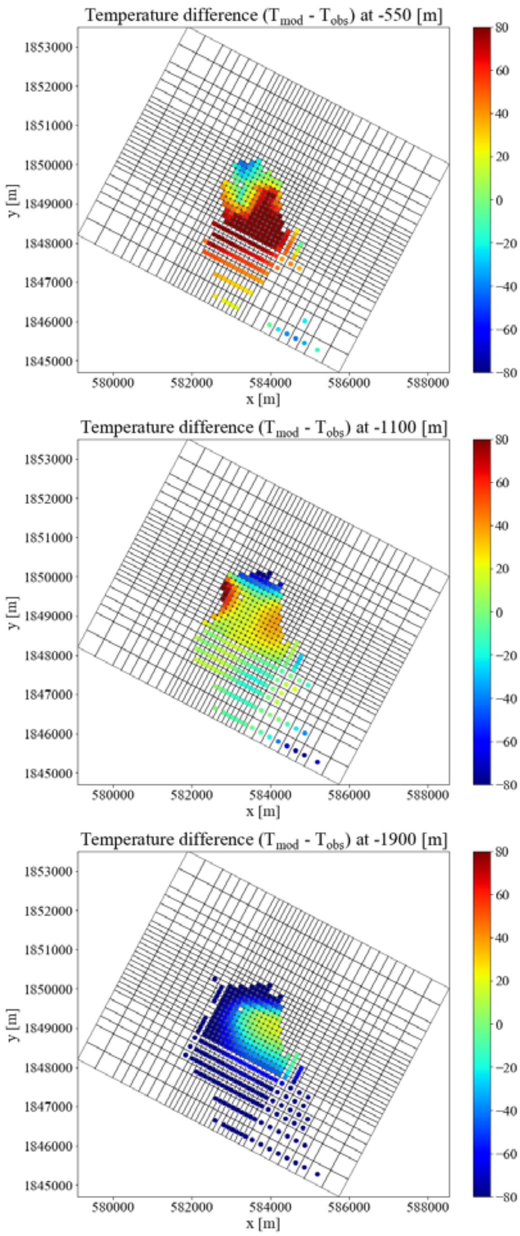

Figure 10: Differences between the results from model MO24535V2 and the seismic temperature data (°C) at three elevations.

4.2 Automatic calibration with iTOUGH2

Some further inversion runs with iTOUGH2 resulted in a reduction of the objective function by ~18% (model MO24535V3). and gave a better match to the inferred seismic temperatures (limited results are shown in Figure 11). After this further automatic calibration with iTOUGH2 it was noted that the vertical permeability of the shallowest rock-types RAAAA and RBBBB showed the greatest sensitivities, i.e., changing their values has the greatest effect on the objective function. In previous inverse modelling studies, we have found that a model can often be improved by subdividing rock-types with high sensitivities, say into a shallow and deep version or an inner and outer version.

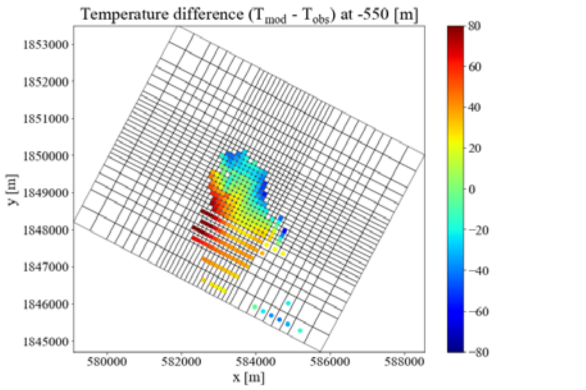

Figure 11: Differences between the model results (MO24535V3), after further calibration with iTOUGH2, and the seismic temperature data (°C) at -550 m.

Also, a review of the geological model given by Sumantoro (2014) showed that there is an uplift across the N-S fault separating the Garibaldi Hill and St George's Hill, also referred to as Fault 2. Based on these ideas an additional rock type, RGGGG, was added just below the sea level on the west side of the model and the other rock types were shifted as shown in Figure 12. These changes were implemented in models MO24535V5 & V6 and were carried forward to the model MO27660 optimised with iWaiwera.

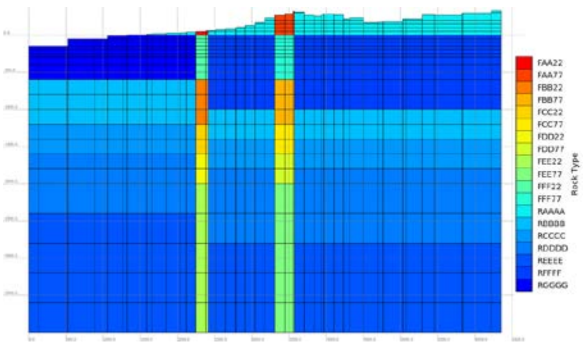

Figure 12: Updated rock-type configuration.

4.3 Automatic calibration using PEST

In parallel with the iTOUGH2 inversions, some PEST automatic calibrations were also carried out. The PEST setup is discussed more fully in (van den Heuvel, 2019).

The singular value decomposition (SVD) option in PEST was turned on by setting SVDMODE to 1.

After 367 forward runs and only one PEST outer iteration, the objective function was reduced by 56% (model MO24535V4). Even with this reduction the results for the match to the seismic temperature are not obviously much better (see Figure 13).

4.4 Automatic calibration using iWaiwera

In order to use iWaiwera, the AUTOUGH2 model had to be made Waiwera compatible. To achieve this compatibility, extra, thinner 25 m layers were introduced near sea level and up to the water table elevation. Then the topography elevation was "snapped" to the top of the closest layer boundary top. The modified model had 40 layers and 27,660 blocks (see Figure 5).

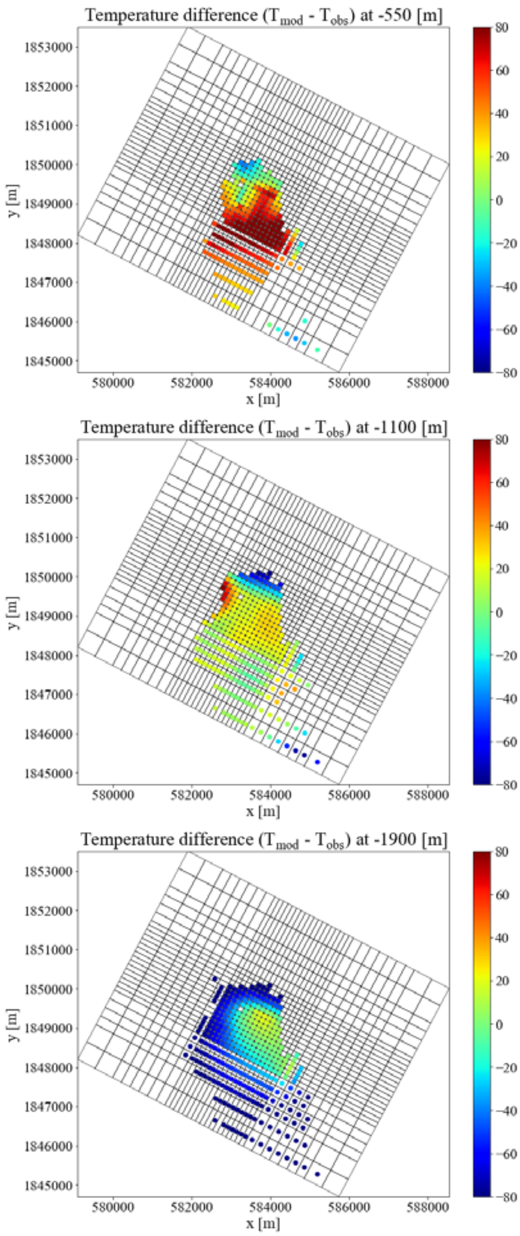

Figure 13: Differences between the model results (model MO24535V4), after calibration with PEST, and the seismic temperature data (°C) at three elevations.

The objective function used with iWaiwera is a variant of (2) with simple regularization defined by:

$$f_p(p) = \|W_2(p - p_*)\|^2 \quad (8)$$

where p_* represents the vector of initial parameter values and W_2 is a diagonal regularization weighting matrix.

Because iWaiwera runs very fast it was possible to carry out many trial inversion runs, varying the regularization parameter α and other parameters. The best result obtained in terms of the seismic temperatures are shown in Figure 14. There are still a few areas where the match could be improved (circled in black) but the results are better than those shown above for iTOUGH2 (Figure 11) or PEST (Figure 13).

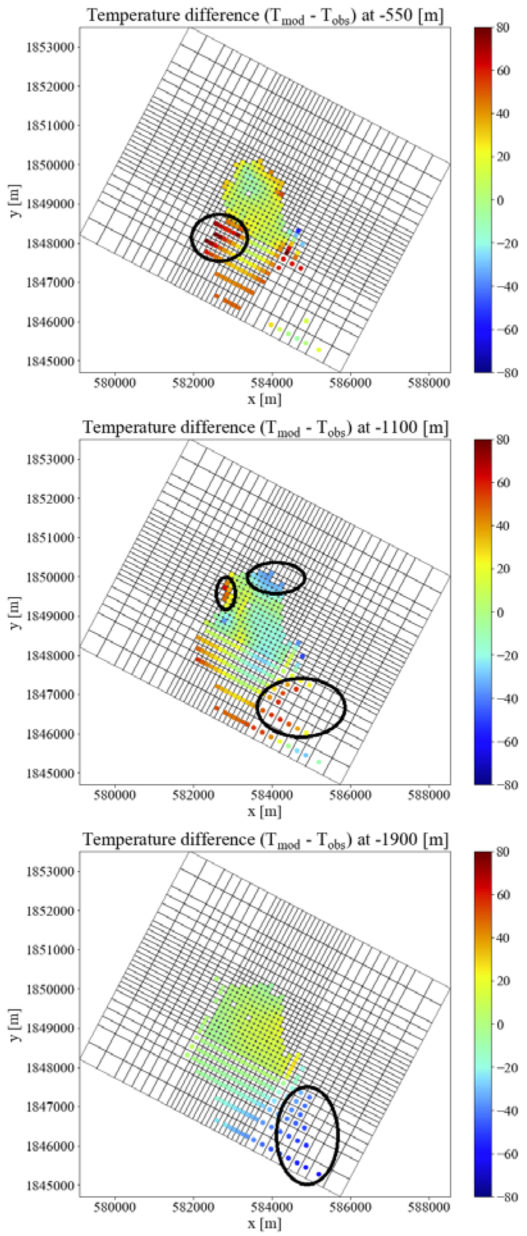

Figure 14: Differences between the model results, after calibration with iWaiwera, and the seismic temperature data (°C) at three elevations.

A comparison of the downhole temperatures for wells Mon-1 and Mon-2 achieved using iTOUGH2, PEST and iWaiwera is shown in Figure 15. The results obtained via iWaiwera, show an improved fit to the wellbore temperature plots, especially for higher elevations. From 0 m to -1000 m, the temperature of the model follows the observed data (almost) perfectly, for both Mon-1 and Mon-2. At depth (say below -1700 m) the iWaiwera model may be too hot but the agreement with the seismic temperatures at -1900 m is very good.

The final check on the model results is the match to the temperatures at the three surface features. The results are shown in Table 3.

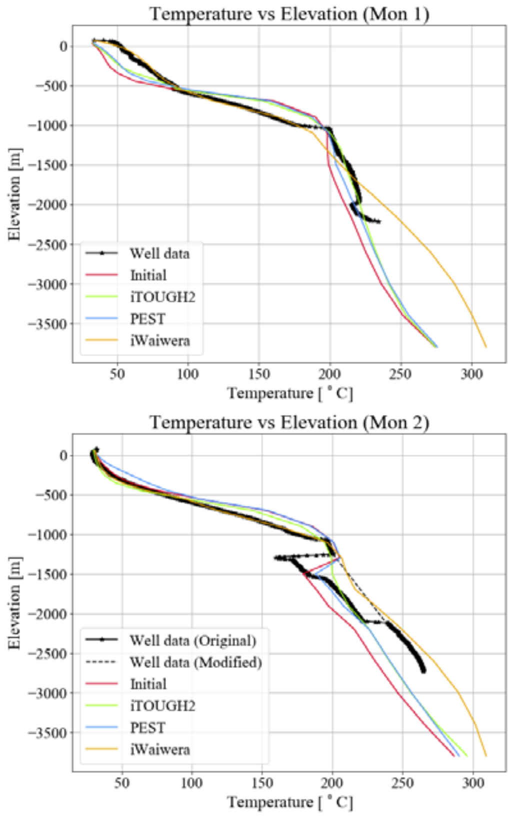

Figure 15: Downhole temperatures for wells Mon-1 and Mon-2 achieved using iTOUGH2, PEST and iWaiwera.

Table 3: Match to temperatures (°C) of surface features.

Column	Data	Initial	iTOUGH2	PEST	iWaiwera
er	59.3	30.3	30.6	30.2	61.3
ew	39.3	107.8	90.0	107.8	39.4
mj	95	29.7	29.7	29.7	30.1

iWaiwera obtained a good fit to the low-elevation hot-spring data but it was not possible to match the surface temperature at the high elevation Gages Soufrière spring 7. It may be necessary to represent this surface feature by a well on deliverability rather than just flow up the model column.

As noted above, the data used for Hot Water Pond may not be correct and the Gages Soufrière spring 7 is now buried. It would be useful to have updated data for surface features to use for model calibration.

4.5 Upflow

The pattern of the deep upflow for the final version of model MO27660 is shown in Figure 16. It shows most of the upflow under St. George's Hill, with some spread along the Fort Ghaut Fault Zone (see Figure 7). These results are consistent with the conceptual model proposed by Ryan et al. (2013) and Ryan & Shalev (2014).

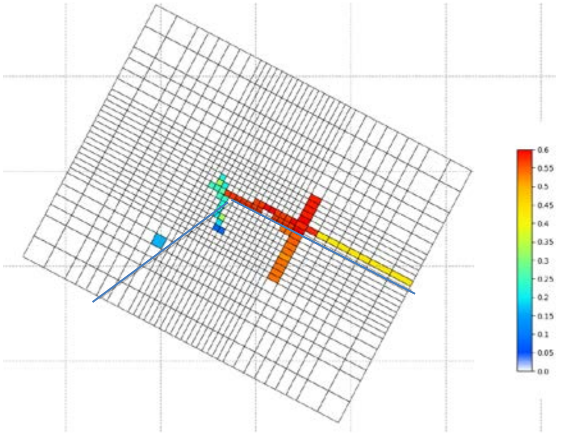

Figure 16: Deep upflows in the best calibrated version of model MO27660 (track shown for the vertical slice in Figure 17).

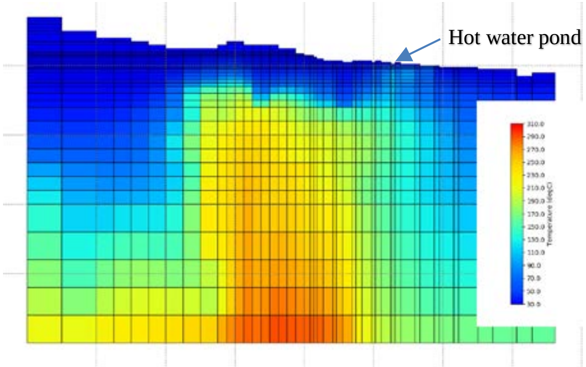

Figure 17: Temperatures along a vertical dog-leg slice (track is shown in Figure 16).

The temperatures along a dog-leg slice are shown in Figure 17. The small out flow towards Hot water Pond can be seen. The calibration did allow the option of a deep upflow even further east, but the inverse modelling process rejected that possibility.

4.6 Improvement of calibration

The progression of inverse modelling started with iTOUGH2 applied to model MO24535V1, producing the improved MO24535V2. The results for MO24535V2 are shown in Figures 8 and 10. The value of objective function for MO24535V1 is given in Table 4 (together with those for other models). The objective function (OF) is the weighted sum of squares of the differences between observed temperatures and model results. The weights chosen were 1.0 for the Mon-1 and Mon-2 downhole temperatures, 0.16 for the seismic inferred temperatures and 10.0 for the three surface temperatures at the hot spring locations. The high weight was used for the surface features to encourage the automatic calibration to take account of the sparse data.

In developing model MO24535V2, several experiments were carried out in setting the parameter bounds and other parameters in iTOUGH2. The experiments with iTOUGH2 settings were successful in reducing the objective function by almost a factor of 2. Next a further iTOUGH2 inversion run (model MO24535V3) and a parallel PEST inversion run (model MO24535V4) were carried out using the parameters from MO24535V2 as the starting point. In the second stage of automatic calibration iTOUGH2 produced a better reduction in the OF than PEST, but this is probably because regularisation was applied with PEST penalizing change from the starting parameter values.

Some modest further reduction to the objective function were made with iTOUGH2 applied to the models with modified permeability structure (models MO24535V5 & V6).

The model MO27660 was sufficiently different to make a direct comparison of the model fit not very useful and therefore results for MO27660 are not included in Table 4.

Table 4: Values of the objective function.

Model	Obj. Funct.	Comments
MO24535V1	12.59E5	Initial version
MO24535V2	6.710E5	After experiments with iTOUGH2
MO24535V3	5.982E5	V2 After more iTOUGH2 calibration
MO24535V4	6,396E5	V2 After PEST calibration
MO24535V5	6.602E5	V2 Modified geology
MO24535V6	5.889E5	V5 After iTOUGH2 calibration

4.7 Problems

Even with the very fast run-time with iWaiwera inverse modelling is still a difficult process. In the above we have presented just the best results and not discussed the many iterations that went into the process. Some of the problems faced are briefly discussed here.

The main difficulty is that some parameters are not well constrained by the data and during inverse modelling their values may be pushed towards upper or lower bounds, possibly leading to an unphysical model, say with a fault permeability much lower than the surrounding formation permeability. This problem can be partly avoided by adjusting upper and lower bounds on some parameters or by applying more regularization through (8), forcing the parameters to stay near their starting values. Singular value decomposition can help but is not yet available in iWaiwera.

5. CONCLUSIONS

With the aid of iWaiwera it was possible to calibrate a natural state model of Montserrat geothermal system to achieve good matches to the observed temperature profiles for wells Mon-1 and Mon-2, and temperatures inferred from the seismic tomography study of Ryan & Shalev (2014). This extra information, based on seismic measurements and inferred from geophysical modelling, was a very valuable addition to the suite of data used for model calibration.

ACKNOWLEDGEMENTS

We thank The Department for International development and the Government of Montserrat for funding aspects of this work and for allowing the use of geothermal drilling and exploration data. We would also like to acknowledge the Campus Research and Publication Fund of The University of the West Indies (CRP.3.JUN15.13) for access to funding.

REFERENCES

Alcaraz, S.A., Lane, R., Spragg, K., Milicich, S.D., Sepulveda, F., Bignall, G.: 3D geological modelling using new Leapfrog Geothermal software. *Proc. 36th Workshop Geothermal Reservoir Engineering*, Stanford University, Stanford, 351–356 (2011).

Bjarkason, E.K., Maclaren, O.J., O'Sullivan, J.P., O'Sullivan, M.J.: Randomized truncated SVD Levenberg-Marquardt approach to geothermal natural state and history matching. *Water Resources Research*, 54, 2376–2404 (2018).

Bjarkason, E.K., O'Sullivan, J.P., Yeh, A., O'Sullivan, M.J.: Combined natural state and history matching using the adjoint or direct sensitivity method. *Proc. 38th New Zealand Geothermal Workshop*, Auckland, New Zealand (2016).

Bjarkason, E.K., O'Sullivan, J.P., Yeh, A., O'Sullivan, M.J.: Inverse modeling of the natural state of geothermal reservoirs using adjoint and direct methods. *Geothermics*, 78, 85–100 (2019).

Bremaud, M.: *Developing a reservoir model of the Montserrat geothermal system, West Indies*. ENSG 3rd year –project report. École Nationale Supérieure de Géologie, Université de Lorraine (2019).

Brophy, P., Poux, B., Suemnicht, G., Hirtz, P., Ryan, G.: Preliminary results of deep geothermal drilling and testing on the island of Montserrat. *Proc. 39th Workshop on Geothermal Reservoir Engineering*, Stanford, California, USA, (2014).

Chiodini, G., Cioni, R., Frullani, A., Guidi, M., Marini, L. Prati, F., Raco, B.: Fluid geochemistry of Montserrat Island, West Indies, *Bull. Volcanol.*, 58(5), 380–392 (1996).

Croucher, A., O'Sullivan, M., O'Sullivan, J., Yeh, A., Burnell, J., Kissling, W.: Waiwera: A parallel open-source geothermal flow simulator. *Computers and Geosciences*, 141 (2020).

Doherty, J.: *Calibration and uncertainty analysis for complex environmental models*. Watermark Numerical Computing, Brisbane, Australia (2015).

Doherty, J.: *Model-Independent Parameter Estimation - User Manual Part I: PEST, SENSAN and Global Optimisers* (7th ed.) Watermark Numerical Computing, Brisbane, Australia (2018a).

Doherty, J.: *Model-Independent Parameter Estimation - User Manual Part II: PEST, Utility Support Software* (7th ed.) Watermark Numerical Computing, Brisbane, Australia (2018b).

EGS Inc.: *Geothermal Exploration in Montserrat, Caribbean*, Final Report. Prepared for the Minister of Communications and Works, Government of Montserrat, Caribbean, 1–11 (2010).

Finsterle, S. (2007). *iTOUGH2 User's Guide*, Report LBNL-40040, Lawrence Berkeley National Laboratory, Berkeley, California, USA.

Finsterle, S. (2015). *iTOUGH2 Command Reference*, Report LBNL-40041 (7th ed.), Lawrence Berkeley National Laboratory, Berkeley, California, USA.

Geotermica Italiana: *Exploration for Geothermal Resources in the Eastern Caribbean*, Rep. TCDCON15/90-RLA/87/037, United Nations Dept. of Technical Cooperation for Development, Pisa, Italy (1991).

Gonzalez-Gutierrez, B., Sung, S., Nicholson, R., O'Sullivan, J.P., O'Sullivan, M.J., Maclaren, O.: Accelerating the solution of geothermal inverse problems using adjoint methods in Waiwera: A progress report. *Proc. 40th New Zealand Geothermal Workshop,* Wairakei, New Zealand (2018).

Kokelaar, B.: Setting, chronology and consequences of the eruption of Soufriere Hills Volcano, Montserrat (1995-1999). *The Eruption of the Soufriere Hills Volcano, Montserrat, From 1995 to 1999,* 1-43. Edited by T. H. Druitt, and B. P. Kokelaar (2002).

Lehuger, U., O'Sullivan, M., O'Sullivan, J., Popineau, J., Ryan, G.A.: Computer modelling of Montserrat geothermal Field. *Proc. 40th New Zealand Geothermal Workshop.* Wairakei, New Zealand (2018).

Pruess, K., Oldenburg, C., Moridis, G.: *TOUGH2 User's Guide, Version 2.0*. Lawrence Berkeley National Laboratory, Berkeley, California (1999).

Rowland, J., Ryan. G.: *Structural Architecture of St George's Hill & Surrounds: Implications for geothermal well siting.* Report: Auckland Uniservices Ltd. (2014)

Ryan, G.A., Peacock, J.R., Shalev, E., Rugis, J.: Montserrat geothermal system: a 3D conceptual model. *Geophysical Research Letters,* 40, 1–6 (2013).

Ryan, G.A., Shalev, E.: Seismic Velocity/Temperature Correlations and a Possible New Geothermometer: Insights from Exploration of a High-Temperature Geothermal System on Montserrat, West Indies. *Energies* 7 (10), 6689–6720 (2014).

Sumantoro, Z.Z.: *Reservoir modelling of the geothermal system in Montserrat*. Project Report, Geothermal Institute, University of Auckland (2014).

van den Heuvel, M.M.M.M.: *Improving a Montserrat geothermal system model by using inverse modelling.* Internship Report, Mechanical Engineering, Eindhoven University of Technology (2019).

Yeh, A., Croucher, A.E., O'Sullivan, M.J.: Recent developments in the AUTOUGH2 simulator. *Proc. TOUGH Symposium*. Lawrence Berkeley National Laboratory, Berkeley, California (2012).

ISSN 2703-4275